

# Sc substitution for Mg in MgB<sub>2</sub>: effects on T<sub>c</sub> and Kohn anomaly

S. Agrestini, C. Metallo, M. Filippi, L. Simonelli, G. Campi, C. Sanipoli

*Dipartimento di Fisica, Università di Roma “La Sapienza”, P. le Aldo Moro 2, 00185 Roma, Italy*

E. Liarokapis

*Department of Applied Mathematics and Physics,  
National Technical University of Athens, GR-157 80 Athens, Greece*

S. De Negri, M. Giovannini, A. Saccone

*Dipartimento di Chimica e Chimica Industriale, Università di Genova, Via Dodecaneso 31, 16146 Genova, Italy*

A. Latini

*Dipartimento di Chimica, Università di Roma “La Sapienza”, P. le Aldo Moro 2, 00185 Roma, Italy*

A. Bianconi

*Unità INFN and Dipartimento di Fisica, Università di Roma “La Sapienza”, P. le Aldo Moro 2, 00185 Roma, Italy*

(Dated: June 20, 2018)

Here we report synthesis and characterization of Mg<sub>1-x</sub>Sc<sub>x</sub>B<sub>2</sub> (0.12<x<0.27) system, with critical temperature in the range of 30>T<sub>c</sub>>6 K. We find that the Sc doping moves the chemical potential through the 2D/3D electronic topological transition (ETT) in the  $\sigma$  band where the “shape resonance” of interband pairing occurs. In the 3D regime beyond the ETT we observe a hardening of the E<sub>2g</sub> Raman mode with a significant line-width narrowing due to suppression of the Kohn anomaly over the range 0<q<2k<sub>F</sub>.

PACS numbers: 74.70.Ad;74.62.Dh;78.30.-j

Following the discovery of superconductivity in MgB<sub>2</sub> with a T<sub>c</sub> of 40 K<sup>1</sup> large attention has been paid to chemical substitutions<sup>2,3,4,5,6,7,8</sup> aiming at enhancement of T<sub>c</sub> and H<sub>c2</sub>, and to manipulate the electronic structure for the understanding of the high T<sub>c</sub> superconductivity. As a matter of fact, chemical substitution in the MgB<sub>2</sub> is difficult and only Al replacing Mg<sup>4,5,6,7</sup> and C replacing B<sup>8</sup> had been successful. Both of these substitutions reduce the T<sub>c</sub> and induce a lattice compression. The variation of T<sub>c</sub> with doping is mostly determined by the tuning of the chemical potential through the electronic topological transition (ETT) where the topology of the Fermi surface of the  $\sigma$  band changes from 2D to 3D<sup>6</sup>. In this two-gap superconductor<sup>9</sup> the exchange-like non-diagonal  $\sigma$ - $\pi$  interband pairing terms that enhance T<sub>c</sub> are expected to exhibit large variation near the ETT<sup>5,6</sup>. In addition, Raman spectroscopy measurements on the Mg<sub>1-x</sub>Al<sub>x</sub>B<sub>2</sub> and MgB<sub>2-x</sub>C<sub>x</sub> systems<sup>10,11,12,13</sup> have revealed a line-width narrowing and energy hardening of the E<sub>2g</sub>-mode with the substitution beyond the ETT. This effect could be interpreted in term of suppression of the Kohn anomaly<sup>14,15</sup> observed over an extended range 0<q<2k<sub>F</sub> in the MgB<sub>2</sub><sup>16,17</sup> by a shift of the Fermi level. In fact the Kohn anomaly<sup>18</sup> is strong (weak) for a 2D (3D) Fermi surface<sup>19,20</sup>. Therefore it is expected to decrease for a 2D to 3D ETT<sup>6,20</sup> of the Fermi surface. The proximity to an ETT has been invoked to explain the anomalous pressure dependence<sup>22</sup> of this mode and it has been proposed to be the driving mechanism for raising the critical temperature<sup>6,23,24</sup>. The aim of this work is to modify the band structure by chemical substitutions

to explore the role of electronic structure in the MgB<sub>2</sub> on the electron-phonon coupling and on T<sub>c</sub> by tuning the chemical potential through the shape resonance.

We have synthesized the new superconducting ternary system Mg<sub>1-x</sub>Sc<sub>x</sub>B<sub>2</sub> for 0.12<x<0.27, where the chemical substitution induces minor lattice variations since the ionic radius of Sc (1.62 Å) is only a little larger than of Mg (1.602 Å). The substituted Sc ions donate 0.12<x<0.27 electrons per unit cell to the conduction  $\sigma$  and  $\pi$  bands so the chemical potential is shifted towards the top of the  $\sigma$  band beyond the ETT<sup>6</sup> where the  $\sigma$  Fermi surface changes from a 2D to a 3D topology, expected near x=0.12<sup>9,18</sup>. Sc substitution for Mg increases the disorder in the Mg/Sc layers but has minor effects on the lattice structure of the boron layer. Therefore the variation of T<sub>c</sub> and electron-phonon coupling with the variation of the electron structure can be well investigated.

In these new samples we observe a remarkable line narrowing and frequency hardening of the E<sub>2g</sub> Raman mode, which gives a compelling experimental evidence for a drastic reduction of the Kohn anomaly and of the electron phonon coupling for x>0.12. It is remarkable to note that the critical temperature in the Mg<sub>1-x</sub>Sc<sub>x</sub>B<sub>2</sub> samples has been dropped only by a factor 2-10 from MgB<sub>2</sub>, much less than expected for a multi-band theory (with doping-independent interband pairing) considering the decrease of the electron-phonon coupling and of the density of states in the  $\sigma$  band. This suggests importance of the resonant enhancement of the interband pairing term<sup>23</sup> and the associated minimum of the non-diagonal coulomb pseudo-potential<sup>24</sup> that drives the T<sub>c</sub>

amplification at the ETT, called “shape resonance” in a two-gap superconductor.

$\text{Mg}_{1-x}\text{Sc}_x\text{B}_2$  samples were synthesized by direct reaction method of the elemental magnesium and scandium (powder, 99.9 mass % nominal purity), boron (99.5 % pure <60 mesh powder). The starting materials were mixed in a stoichiometric ratio and pressed into pellets of 8 mm in diameter. Each pellet was enclosed in a tantalum crucible and sealed by arc welding under argon atmosphere. The Ta crucibles were then heated in a furnace Centorr M60 under high-pure Ar atmosphere for 14 hours in the temperature range between 1280 and 950 °C.

The phase purity of the samples was checked by X-ray diffraction. The diffraction patterns of  $\text{Mg}_{1-x}\text{Sc}_x\text{B}_2$  samples were measured in the Bragg-Brentano  $\theta$ - $\theta$  geometry by a vertical X’Pert Pro MPD diffractometer using a Cu  $K_\alpha$  radiation. The X-ray diffraction measurements of several samples were repeated at the beamline ID31 of the European Synchrotron Radiation Facility (ESRF), Grenoble. The samples were sealed in 1.0 mm diameter glass capillaries and the high-resolution diffraction profiles ( $\lambda=0.5 \text{ \AA}$ ) were collected at  $T=80 \text{ K}$  using nine Ge(111) analyzer crystals. The reflections were indexed to a  $\text{MgB}_2$ -like structure according to the hexagonal  $\text{AlB}_2$  structure type (P6/mmm space group). No Sc,  $\text{Sc}_2\text{O}_3$  or  $\text{ScB}_{12}$  minority phases were found, which indicates a successful Sc substitution for Mg. Figure 1a shows profiles of (002) and (110) diffraction peaks for representative sample of the  $\text{Mg}_{1-x}\text{Sc}_x\text{B}_2$  system. A line broadening is observed in Sc-doped compounds as compared to  $\text{MgB}_2$  and  $\text{ScB}_2$  indicating disorder or non-uniformities due to Mg/Sc layers.

The samples were characterized for their superconducting properties by the temperature dependence of complex conductivity using the single-coil inductance method<sup>5,6</sup>. The temperature dependent radio-frequency complex conductivity for representative Sc contents is shown in Fig. 1b where it can be seen that the introduction of Sc in the Mg-planes induces a clear shift of the superconducting transition to lower temperatures. The superconducting transition for the Sc-doped samples shows a broadening. This indicates that some disorder does exist in the Sc-doped samples with possible effect on the superconductivity via an increase of intraband scattering in the  $\pi$  band.

The Raman spectra were measured in the back-scattering geometry, using a T64000 Jobin-Yvon triple spectrometer with a charge-coupled device camera. The explored Raman shift ranges between 200 and 1100  $\text{cm}^{-1}$ . The 488.0 nm  $\text{Ar}^+$  laser line was focused on 1-2  $\mu\text{m}$  large crystallites and the power was kept below 0.03 mW to avoid heating by the beam. Typical spectra recorded for selected temperatures are shown in Fig. 1c. The in-plane Boron vibration with  $E_{2g}$  symmetry produces a single narrow peak in Raman spectrum of  $\text{ScB}_2$  as in  $\text{AlB}_2$ <sup>10,12</sup> also if at lower energy according with its larger lattice parameters. The Raman line is softened going from  $\text{ScB}_2$

to  $\text{Mg}_{1-x}\text{Sc}_x\text{B}_2$  and finally becomes very soft and very broad in  $\text{MgB}_2$ .

The diffraction data were analyzed by Rietveld refinement using GSAS program. The behaviour of the lattice parameters  $a$  and  $c$  as a function of Sc content is reported in Fig. 2. A miscibility gap occurs in the range from  $2\pm 1\%$  to  $12\pm 1\%$  Sc substitution where the samples show a macroscopic phase separation between low-doped and high-doped samples. The  $a$ -axis increases gradually with increasing Sc-content, while the  $c$ -axis is nearly constant. The unit cell volume shows a small expansion in agreement with the similar ionic radius between  $\text{Sc}^{3+}$  and  $\text{Mg}^{2+}$ . For comparison in the same figure we report the evolution of the lattice parameters in the  $\text{Mg}_{1-x}\text{Al}_x\text{B}_2$  system that shows much larger lattice variations. Here “ $x$ ” is the nominal Sc-content and we can conclude that the introduced Sc is successfully substituted for Mg, and the actual Sc-content is not much different from the nominal value. From the variation of lattice parameters with Sc content, we can conclude that the solubility range of Scandium in  $\text{MgB}_2$  is between 12% and 27%.

The variation of the superconducting critical temperature  $T_c$  as a function of Sc doping is reported in the panel (a) of Fig. 3. The transition temperature  $T_c$  was determined from the peak in derivative of the complex conductivity. The  $T_c$  decreases continuously with increasing Sc substitution from 30K at 12% to 6K at 27%. It is interesting to note that the variation of  $T_c(x)$  is sharper for  $0.12 < x < 0.15$ .

The panel (b) of Fig. 3 shows the variation of the frequency of the  $E_{2g}$  Raman line from  $\text{MgB}_2$  to  $\text{Mg}_{1-x}\text{Sc}_x\text{B}_2$ . The error bars indicate the  $E_{2g}$  peak half-width. In the Sc-substituted samples in the range 12%-27% the phonon peak is shifted toward higher frequency, it is much narrower in comparison with  $\text{MgB}_2$  and it is approaching the frequency of that for the  $\text{ScB}_2$ . The frequency hardening and the line-width narrowing of the Raman  $E_{2g}$  mode indicates a clear decrease of the electron-phonon coupling going from  $\text{MgB}_2$  to the Sc-doped samples.

Finally in Fig. 4 we report the energy of the Raman  $E_{2g}$  mode as a function of the  $a$ -axis (that is the relevant parameter for the in plane high frequency longitudinal optical mode  $E_{2g}$ ) of the non-superconducting diborides  $\text{ScB}_2$  and  $\text{AlB}_2$ , and of the superconducting  $\text{MgB}_2$ ,  $\text{Mg}_{1-x}\text{Sc}_x\text{B}_2$  and  $\text{Mg}_{0.5}\text{Al}_{0.5}\text{B}_2$ <sup>13</sup> systems.

Let us consider first the  $\text{AlB}_2$  and  $\text{ScB}_2$  samples with a filled  $\sigma$  band. The energy of the  $E_{2g}$  mode as a function of  $a$ -axis follows the law  $\Omega(a) = \omega_{Al}(a/a_{Al})^{-3\gamma_{0a}}$  (dashed line in panel a) where  $\gamma_{0a}$  is the Gruneisen parameter  $\gamma_{0a} = -\partial \ln \nu / 3 \partial \ln a = 1.4 \pm 0.1$  that is the expected behaviour due to lattice expansion for a metallic covalent material.

In the case where the Fermi level is tuned below the top of the  $\sigma$  band (e.g.  $\text{MgB}_2$ ,  $\text{Mg}_{1-x}\text{Sc}_x\text{B}_2$  and  $\text{Mg}_{0.5}\text{Al}_{0.5}\text{B}_2$ ) a phonon decay channel opens up unlike others with filled  $\sigma$  band (e.g.  $\text{AlB}_2$  and  $\text{ScB}_2$ ). In fact the phonons can now decay into electron-hole exci-

tations in the  $\sigma$  band inducing a phonon energy softening and line broadening (Kohn anomaly). The  $E_{2g}$  phonon softening can be obtained by the energy difference between the experimental  $E_{2g}$  Raman energy  $\omega_{E_{2g}}$  and the expected phonon energy  $\Omega_{E_{2g}}(a)$  for a material with a filled  $\sigma$  band and with the appropriate lattice parameter. We deduce the large phonon softening of 37 meV for  $\text{MgB}_2$  and about 17 meV for  $\text{Mg}_{1-x}\text{Sc}_x\text{B}_2$  system that is close to the case of  $\text{Mg}_{0.5}\text{Al}_{0.5}\text{B}_2$ . The Raman softening in  $\text{MgB}_2$  is due to large electron-phonon interaction with the electron-hole excitations in the  $\sigma$  band that drives the system close to a lattice instability and the breakdown of Migdal approximation<sup>9,18</sup>. The decrease of the electron-phonon coupling near  $q=0$  going from  $\text{MgB}_2$  to  $\text{Mg}_{1-x}\text{Sc}_x\text{B}_2$  is given by the variation of the ratio  $(\Omega_{E_{2g}}(q=0)/\omega_{E_{2g}}(q=0))^2$  shown in panel (b) going from 2.2 in  $\text{MgB}_2$  to 1.4 in  $\text{Mg}_{0.8}\text{Sc}_{0.2}\text{B}_2$ . This drastic decrease is related to a smaller  $E_{2g}$  Kohn anomaly in  $\text{Mg}_{1-x}\text{Sc}_x\text{B}_2$ . This result is confirmed by the variation of the ratio between the line-width and the phonon energy  $2\gamma/\omega_{E_{2g}}$  shown in panel c of Fig. 4 that decreases going from  $\text{MgB}_2$  to  $\text{Mg}_{0.8}\text{Sc}_{0.2}\text{B}_2$ . These results can be understood if the Sc substitution has driven the chemical potential through the ETT where the  $\sigma$  Fermi surface has a 3D topology<sup>6</sup> with a reduced Kohn anomaly<sup>14,15</sup>.

In conclusion we have reported the successful substitution of Sc for Mg with  $0.12 < x < 0.27$  obtaining a very small lattice expansion. The system shows a miscibility gap in the range  $0.02 < x < 0.12$ , which supports the fact that the system is in the proximity of a lattice instability expected at the 2.5 Lifshitz phase transition<sup>21</sup> in agreement with pressure effect measurements<sup>22</sup>. The effect of the Sc doping is to shift the chemical potential toward the ETT and the top of the  $\sigma$  band. However the rigid band model is not appropriate since we expect that the

Sc substitution increases the  $sp^2(\text{B})\text{-d}(\text{Sc})$  hybridization and the dispersion of the  $\sigma$  band.

In the  $\text{Mg}_{1-x}\text{Sc}_x\text{B}_2$  samples the  $E_{2g}$  Raman mode shows a large hardening and narrowing in comparison with  $\text{MgB}_2$  while the lattice expands, that indicates a drastic reduction of the Kohn anomaly in the  $E_{2g}$  longitudinal optical mode. This effect has been associated with the tuning of the Fermi level beyond the critical energy for the ETT where the two dimensional topology of the  $\sigma$  Fermi surface changes to a three dimensional topology. The critical temperature in the  $\text{Mg}_{1-x}\text{Sc}_x\text{B}_2$  samples has been found in the range 30-6 K as in the case of Al substituted samples in the regime where the Fermi surface of the  $\sigma$  band has a 3D topology beyond the 2D/3D ETT<sup>6</sup>. The high values of  $T_c$  in this multi-band superconductor are associated with the key role of the non-diagonal inter-channel pairing term and coulomb pseudo-potential term as in the case of Al substitution<sup>23,24</sup>. These new data support the key role of the electronic structure controlling the resonant enhancement of the exchange like interband coupling term in a two-gap superconductor. This occurs when the chemical potential is tuned in an energy window around the 2D/3D electronic topological transition in one of the two Fermi surface portions giving the shape resonance<sup>25</sup> that pushes up the critical temperature.

We thank the ESRF for provision of synchrotron radiation facilities and we would like to thank Prof. A. Fitch and Dr. I. Margiolaki for assistance in using beamline ID31. We thank R. de Coss for useful discussions. This work was supported by MIUR in the frame of the project Cofin 2003 ‘‘Synthesis and properties of new borides’’, by ‘‘Istituto Nazionale Fisica della Materia’’ (INFM), and by ‘‘Consiglio Nazionale delle Ricerche’’ (CNR) in the frame of the project 5% ‘‘Applicazioni della superconduttività ad alte  $T_c$ ’’ law 95/95.

<sup>1</sup> J. Nagamatsu, N. Nakagawa, T. Muranaka, Y. Zenitani, and J. Akimitsu, *Nature* **410**, 63 (2001).

<sup>2</sup> C. Buzea and T. Yamashita, *Supercond. Sci. Technol.* **14**, R115 (2001).

<sup>3</sup> R. J. Cava, H. W. Zandbergen, and K. Inumaru, *Physica C* **385**, 8-15(2003).

<sup>4</sup> J. S. Slusky, N. Rogado, K. A. Regan, M. A. Hayward, P. Khalifah, T. He, K. Inumaru, S. Loureiro, M. Haas, H. W. Zandbergen, and R. J. Cava, *Nature* **410**, 343 (2001).

<sup>5</sup> S. Agrestini, D. Di Castro, M. Sansone, N. L. Saini, A. Saccone, S. De Negri, M. Giovannini, M. Colapietro, A. Bianconi, *J. Phys.: Condens. Matter* **13**, 11689 (2001).

<sup>6</sup> A. Bianconi, D. Di Castro, S. Agrestini, G. Campi, N. L. Saini, A. Saccone, S. De Negri and M. Giovannini, *J. Phys.: Condens. Matter* **13**, 7383 (2001); A. Bianconi, D. Di Castro, S. Agrestini, G. Zangari and N. L. Saini, A. Saccone, S. De Negri, M. Giovannini G. Profeta, A. Continenza, G. Satta, S. Massidda, A. Cassetta, A. Pifferi, M. Colapietro, *Phys. Rev. B* **65**, 174515 (2002).

<sup>7</sup> J. Q. Li, L. Li, F. M. Liu, C. Dong, J. Y. Xiang, and Z. X. Zhao, *Phys. Rev. B* **66**, 012511 (2002).

<sup>8</sup> S. Lee, T. Masui, A. Yamamoto, H. Uchiyama and S. Tajima, *Physica C* **397**, 7 (2003); S. M. Kazakov, J. Karpinski, J. Jun, P. Geiser, N.D. Zhigadlo, R. Puzniak, A.V. Mironov, *cond-mat/0304656*.

<sup>9</sup> I. I. Mazin, and V. P. Antropov, *Physica C* **385**, 49 (2003).

<sup>10</sup> K.-P. Bohnen, R. Heid, and B. Renker, *Phys. Rev. Lett.* **86**, 5771 (2001).

<sup>11</sup> P. Postorino, A. Congeduti, P. Dore, A. Nucara, A. Bianconi, D. Di Castro, S. De Negri and A. Saccone, *Phys. Rev. B* **65**, 020507 (2001).

<sup>12</sup> B. Renker, K. B. Bohnen, R. Heid, and D. Ernst, H. Schober and M. Koza P. Adelman, P. Schweiss, and T. Wolf, *Phys. Rev. Lett.* **88**, 067001 (2002).

<sup>13</sup> D. Di Castro, S. Agrestini, G. Campi, A. Cassetta, M. Colapietro, A. Congeduti, A. Continenza, S. De Negri, M. Giovannini, S. Massidda, M. Nardone, A. Pifferi, P. Postorino, G. Profeta, A. Saccone, N. L. Saini, G. Satta, A. Bianconi, *Europhys. Lett.* **58**, 278 (2002).

<sup>14</sup> G. Grüner, ‘‘Density Waves in solids’’ Perseus Publ., Cambridge, Massachusetts 2000).

<sup>15</sup> M. E. Flatté, *Phys. Rev.* **50**, 1190 (1994).

- <sup>16</sup> A. Shukla, M. Calandra, M. d'Astuto, M. Lazzeri, F. Mauri, C. Bellin, M. Krisch, J. Karpinski, S. M. Kazakov, J. Jun, D. Daghero, and K. Parlinski, *Phys. Rev. Lett.* **90**, 095506 (2003).
- <sup>17</sup> A.Q.R. Baron, H. Uchiyama, Y. Tanaka, S. Tsutsui, D. Ishikawa, S. Lee, R. Heid, K.-P. Bohnen, S. Tajima, T. Ishikawa, *cond-mat/0309123* (2003).
- <sup>18</sup> W. E. Pickett, *Brazilian Journal of Physics* **33**, 695 (2003); J. M. An, S. Y. Savrasov, H. Rosner, and W. E. Pickett, *Phys. Rev. B* **66**, 220502-R (2002); W. E. Pickett, J. M. An, H. Rosner, and S. Y. Savrasov, *Physica C* **387**, 117 (2003) and references therein.
- <sup>19</sup> S. Tsuda, T. Yokoya, Y. Takano, H. Kito, A. Matsushita, F. Yin, J. Itoh, H. Harima, and S. Shin, *Phys. Rev. Lett.* **91**, 12700 (2003).
- <sup>20</sup> A. Carrington, P. J. Meeson, J. R. Cooper, L. Balicas, N. E. Hussey, E. A. Yelland, S. Lee, A. Yamamoto, S. Tajima, S. M. Kazakov, and J. Karpinski, *Phys. Rev. Lett.* **91**, 037003 (2003).
- <sup>21</sup> I. M. Lifshitz, *Soviet Physics JEPT* **11**, 1130 (1960).
- <sup>22</sup> A. F. Goncharov, V. V. Struzhkin, *Physica C* **385** 117 (2003).
- <sup>23</sup> A. Bussmann-Holder and A. Bianconi, *Phys. Rev. B* **67**, 132509 (2003).
- <sup>24</sup> G. A. Ummarino, R. S. Gonnelli, S. Massidda, A. Bianconi, *Physica C* **407** 121 (2004).
- <sup>25</sup> A. Bianconi, A. Valletta, A. Perali and N. L. Saini, *Physica C* **296**, 269 (1998).

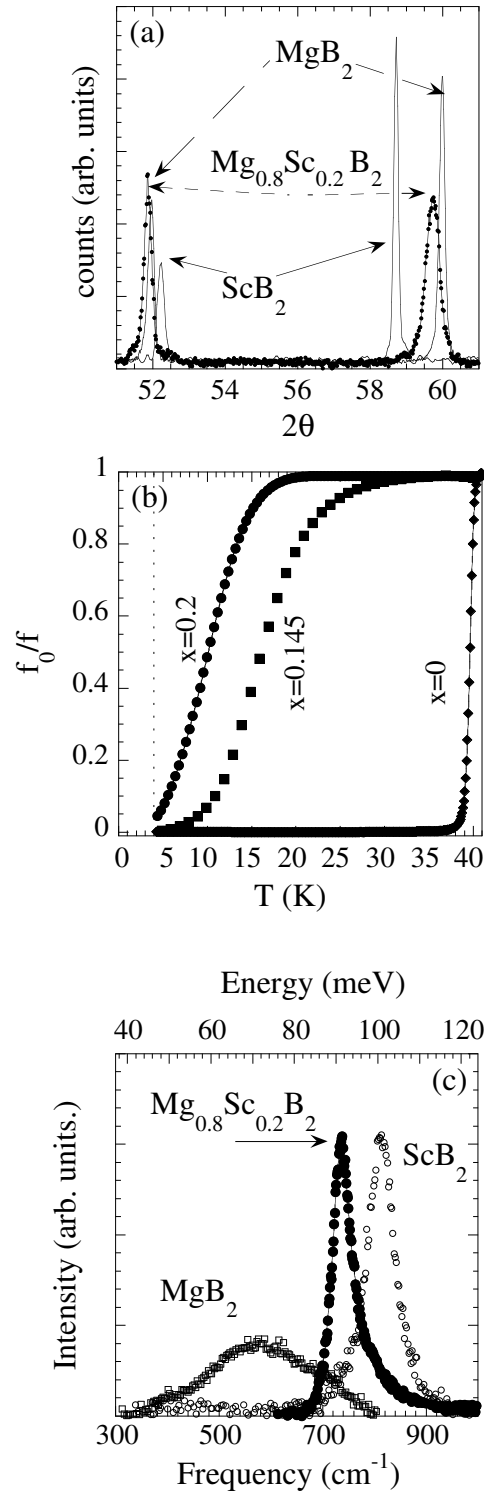


FIG. 1: The X-ray diffraction patterns in the range of the (001) and (110) reflections (panel a), the superconducting transition measured by complex resistivity (panel b), and the Raman spectra (panel c) are shown for representative  $\text{Mg}_{1-x}\text{Sc}_x\text{B}_2$  samples compared with  $\text{MgB}_2$  and  $\text{ScB}_2$ .

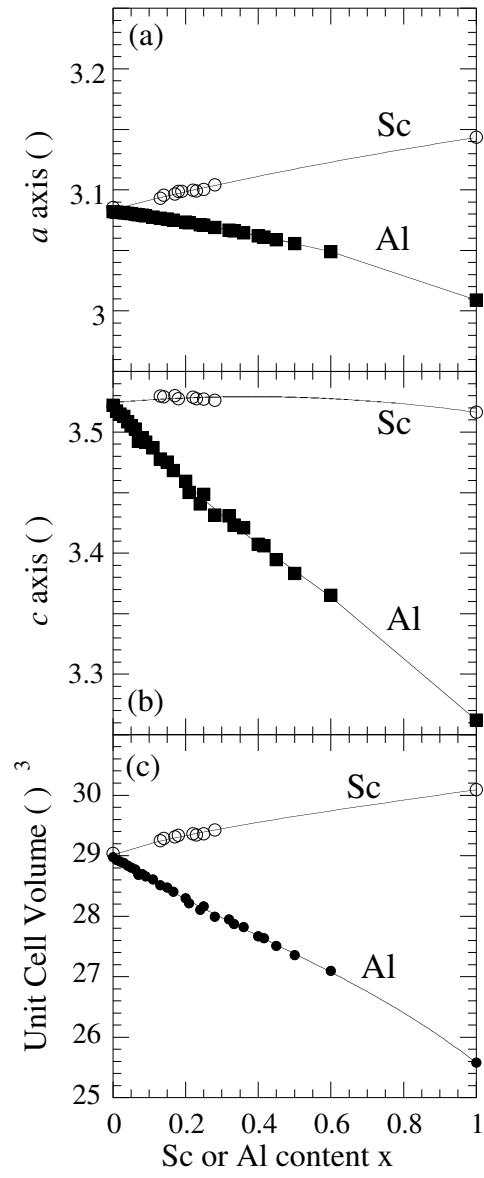


FIG. 2: Changes of lattice parameters  $a$  (panel a) and  $c$  (panel b) and of unit cell volume (panel c) as a function of Sc content  $x$  in  $\text{Mg}_{1-x}\text{Sc}_x\text{B}_2$ .

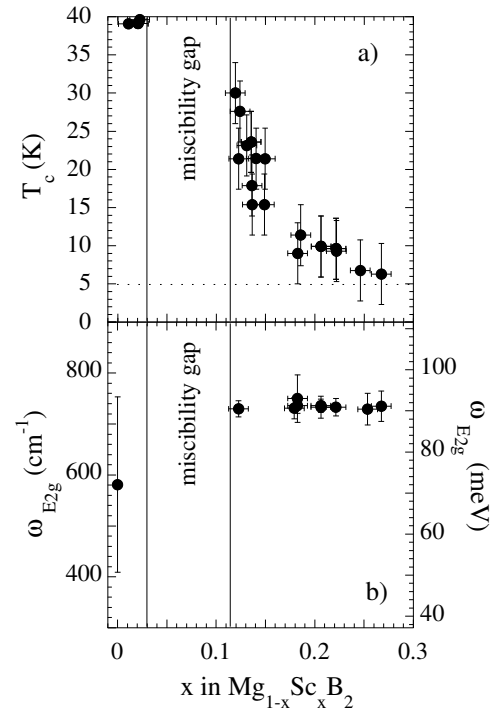


FIG. 3: Evolution of the superconducting critical temperature  $T_c$  (panel a), the frequency  $\omega_{E_{2g}}$  (panel b) of the  $E_{2g}$  Raman line as a function of  $x$  in  $\text{Mg}_{1-x}\text{Sc}_x\text{B}_2$ . The superconductive transition width and the  $E_{2g}$  peak half-width are indicated as error bars respectively in panel a and panel b.

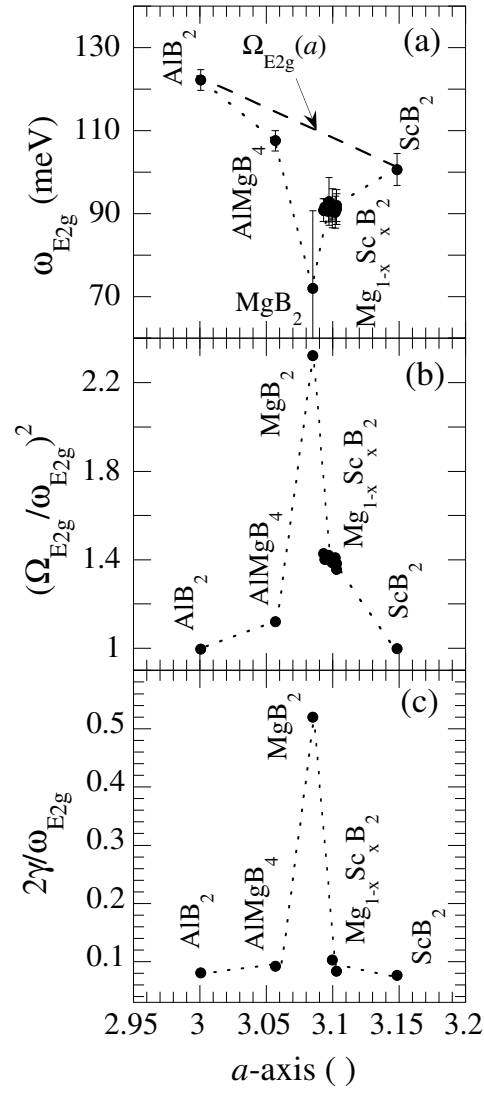


FIG. 4: Variation of the frequency of the  $E_{2g}$  Raman line as function of the lattice parameter  $a$  for different diborides (panel a). The softening and broadening of the  $E_{2g}$  mode due to the Kohn anomaly is given by the energy ratio  $(\Omega_{E_{2g}}(a)/\omega_{E_{2g}}(a))^2$  (panel b) and the ratio  $2\gamma/\omega_{E_{2g}}$  (panel c) where  $2\gamma$  is the Raman line-width.